www.czasopisma.pan.pl PAN www.journals.pan.pl
Archives of Acoustics Vol. 47, No. 4, pp. 555–564 (2022), doi: 10.24425/aoa.2022.142891

Research Paper

Asymmetrical PZT Applied to Active Reduction of Asymmetrically Vibrating Beam – Semi-Analytical Solution

Adam BRAŃSKI, Romuald KURAS*

Laboratory of Acoustics, Department of Electrical and Computer Engineering Fundamentals
Rzeszow University of Technology
Rzeszow, Poland

*Corresponding Author e-mail: r.kuras@prz.edu.pl

(*received September 21, 2021; accepted June 12, 2022*)

The article extended the idea of active vibration reduction of beams with symmetric modes to beams with asymmetric modes. In the case of symmetric modes, the symmetric PZT (s-PZT) was used, and the optimization of the problem led to the location of the s-PZT centre at the point with the greatest beam curvature. In the latter case, the asymmetric modes that occur due to the addition of the point mass cause an asymmetric distribution of the bending moment and transversal displacement of a beam. In this case, the optimal approach to the active vibration reduction requires both new asymmetric PZT (a-PZT) and its new particular distribution on the beam. It has been mathematically determined that the a-PZT asymmetry point (a-point), ought to be placed at the point of maximum beam bending moment. The a-PZT asymmetry was found mathematically by minimizing the amplitude of the vibrations. As a result, it was possible to formulate the criterion of the maximum bending moment of the beam. The numerical calculations confirmed theoretical considerations. So, it was shown that in the case of asymmetric vibrations, the a-PZTs reduced vibrations more efficiently than the s-PZT.

Keywords: beam; actuator (PZT); active vibration reduction; vibration reduction coefficient; effectiveness coefficient.

1. Introduction

The active reduction of the structure vibration is realized with piezoelectric actuators (Hansen, Snyder, 1997; Fuller *et al.*, 1997). The efficiency of reduction depends on two main parameters. First of them is the distribution of PZT on the structure. The second one is the geometric and physical quantities of the PZT. To obtain the best vibration reduction efficiency, both parameters should be optimized. Up to now, many articles based on different ideas have considered these topics, but all were dealt with symmetrical PZTs and symmetrical modes. There are two main approaches to these problems, i.e. exact and numerical approaches.

Exact analytical approach is used in (Barboni *et al.*, 2000) to find an optimal placement of symmetrical PZT on the flexural beam with various boundary conditions. The review of mathematical modelling of actively controlled piezo smart structures is presented by Gupta *et al.* (2011). This problem was also solved in (Brański, Lipiński, 2011; Brański, 2011; 2013) using s-PZTs; the position of the internal activity point was in the centre of s-PZT. It was shown that the most effective location of s-PZT occurred in subdomains with the largest curvatures and this location was called optimal. The criterion was named as the criterion of maximal curvature. The optimal distribution of s-PZTs was deduced on the basis of heuristic premises and strictly confirmed theoretically. The above criterion which is right for a symmetrical structure, is not valid for asymmetrical structures.

As part of the numerical approach, Hu and Li (2018) used genetic algorithm to improve the performance of multi-mode vibration control in cylindrical shells; the position, size and rotation angle of the actuator were chosen as the optimization parameters. Zhang *et al.* (2018) investigated the optimization,

as a part of topology theory, of the electrode coverage over actuators attached to a thin-shell structure to reduce energy consumption of the system. Yassin *et al.* (2018) presented a hybrid optimization approach based on a genetic algorithm, sequential quadratic programming and particle swarm optimization combined with a projected gradient techniques; the location of the actuator centre and shape orientation were chosen as optimization variables. Zorić *et al.* (2019) studied optimization of position, size and orientation of the actuators based on the Gramian controllability matrix using particle swarm optimized self-tuning fuzzy logic controller. Brand and Cole (2020) proposed optimal actuator placement for controlling flexural vibration of a thin rotating ring using cost function based on time-weighted controllability Gramian. There are also articles that numerically confirm the relationship between the beam bending moment and the optimal location of the PZT (Augustyn *et al.*, 2014; Fawade *et al.*, 2016). Fawade *et al.* (2016) investigated the location of the PZT in three different places along the length of the cantilever beam, the best result was obtained when the actuator was closest to the fixed edge, i.e. in the location where the beam bending moment reaches maximum for the given boundary conditions.

In all the articles mentioned above, both in the strict and numerical approach, the influence of PZT asymmetry and its position on the effectiveness of the vibration reduction was not considered. Neither precisely, mathematically justified, optimal these values were indicated. Furthermore, numerical approaches do not have an exact theory. Therefore, it is not possible to precisely point out the geometrical and physical parameters of PZT and its location on the structure based on the structure vibrations, so as to ensure maximum efficiency of the vibration reduction. It seems that this paper fills this gap in the problem of the active vibration reduction, at least for one-dimensional structures such as a beam.

Thus, the aim of this paper is to formulate a new criterion that would indicate the optimal distribution of a-PZT on an asymmetrical structure. To achieve the aim, asymmetric vibrations of the beam caused by additional concentrated mass were considered (Brański, 2011; 2012). It is assumed that the beam is excited by concentrated harmonic force with the first three modes separately. Furthermore, the results of the research in (Brański, 2013) are taken into account, i.e. it is more effective to use one s-PZT than several s-PZTs. With the above assumptions, a semi-analytical formula was derived for the maximum reduction of vibrations. From this formula follows the a-PZT asymmetry and its position on the beam (determined via a-point). The asymmetry of the a-PZT means that the forces on opposite edges have different values and the a-point is not in the centre of a-PZT. Determining of the a-point leads to the determining different arms of forces on opposite edges. The values of these forces, or more precisely the values of the respective pairs of forces, were determined assuming that the asymmetric moments of both pairs of forces are equal. The effect of acting of the a-PZT is measured by the reduction of vibration amplitude which translates into reduction of the vibration, bending moment and shear force. The results were compared to the results of s-PZT. It was assumed that the dimensions a-PZT and s-PZT are the same and in both cases the amounts of energy added to the systems are identical.

The considered examples confirm the effectiveness of the new criterion. To the authors' knowledge, such problem has not been considered yet.

2. Forced vibration of the set beam-mass-actuator

The beam structure consists of a beam and a concentrated mass. Whereas the beam structure and the PZT constitute a mechanical set beam-mass-actuator (BMA). As far as concentrated mass, its addition ensures asymmetrical vibrations of the beam structure. A beam simply supported at both ends was considered (Khasawneh, Segalman, 2019), Fig. 1. The BMA structure vibration equation is given by (Brański, 2011; Dhuri, Seshu, 2006; Kasprzyk, Wiciak, 2007; Filipek, Wiciak, 2008):

$$EJD^4u + (\rho S + \alpha_m)\, D_t^2 u = -f, \tag{1}$$

where

$$\begin{aligned} EJ &= E_bJ_b + E_aJ_a \langle H\rangle^0, \\ \rho S &= \rho_b S_b + \rho_a S_a \langle H\rangle^0, \\ \alpha_m &= m\delta(x - x_m). \end{aligned} \tag{2}$$

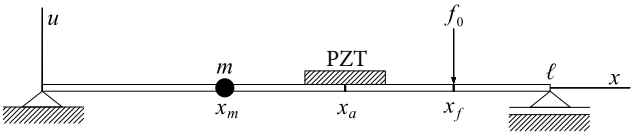

Fig. 1. Geometry of the problem.

Symbols E, J, h, ρ, S mean the physical and geometrical parameters of the beam, actuators, i.e. Young's modulus, surface moment of inertia, thickness, mass density, surface of the rectangular cross-section, respectively. Furthermore, some symbols are supplemented with the following index b, a, m = [b]eam, [a]ctuator, [m]ass, and ℓ – length of the beam, $S = h_1h_2$, h_1 – width, h_2 – thickness, $f = f(x,t)$ – excited force, $u = u(x,t)$ – transversal displacement of a beam at the point x and at the moment t, $D_x^4(...) = \partial^4(...)/\partial x^4$, $D_t^2(...) = \partial^2(...)/\partial t^2$, $\langle H\rangle^0 = H(x_1 - x_2) = H(x - x_1) - H(x - x_2)$, $H(x - x_1)$ – the Heaviside step function in point x_1, and so on.

Boundary conditions are described by the following equations:

$$u(x,t) = 0, \quad x = 0, \quad D_x^2 u(x,t) = 0, \quad x = 0, \tag{3}$$

$$u(x,t) = 0, \quad x = \ell, \quad D_x^2 u(x,t) = 0, \quad x = \ell. \tag{4}$$

Initial conditions are assumed to be zero. Let be the excited force in the form (Kozień, 2013):

$$f(x,t) = f_0 \exp(i\omega_f t)\delta(x - x_f), \tag{5}$$

where $i = (-1)^{1/2}$, ω_f is excited frequency, f_0 is amplitude of the force.

2.1. Eigenvalue problem

To this end, in Eq. (1) it is assumed that $f = 0$. In addition, the actuator is omitted, assuming that its weight and rigidity are small compared to the beam and concentrated mass. According to Eq. (2) one has $EJ = E_b J_b$ and $\rho S = \rho_b S_b$. For harmonic vibrations Eq. (1) leads to:

$$D^4 X_j - \lambda_j^4 X_j = 0, \tag{6}$$

where $j = \{1, 2\}$ is the number of elements of the beam, $DX_j \equiv D_x X_j$, $D^4 X_j \equiv D_x^4 X_j$, and so on.

The dispersion relationship is given by

$$\lambda_j^4 = \omega^2(\rho_j S_j)/(E_j J_j) = \omega^2/\gamma_j$$

and taking into account the above assumptions is $\lambda_1 = \lambda_2 = \lambda$.

It is convenient to present the solution to Eq. (6) in local coordinates, i.e. in $x \in [0, e_j]$; in the separate j-element the solution has the form, Fig. 2:

$$X_j(x) = a_j K_1(\lambda_j x) + b_j K_2(\lambda_j x) + c_j K_3(\lambda_j x) + d_j K_4(\lambda_j x), \tag{7}$$

where Krylov functions $K_\kappa(.)$, $\kappa = \{1, 2, 3, 4\}$ may be found anywhere, e.g. (Kaliski, 1986).

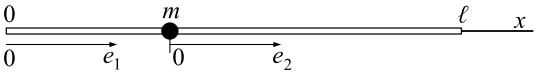

Fig. 2. Geometry of the beam structure in local coordinates.

Boundary conditions have the form:

- at the left end of the 1st element:

$$X_1(0) = 0, \qquad D^2 X_1(0) = 0; \tag{8}$$

- between 1st and 2nd elements:

$$X_1(\lambda_1 e_1) = X_2(\lambda_2 0),$$
$$DX_1(\lambda_1 e_1) = DX_2(\lambda_2 0),$$
$$E_1 J_1 D^2 X_1(\lambda_1 e_1) = E_2 J_2 D^2 X_2(\lambda_2 0),$$
$$E_1 J_1 D^3 X_1(\lambda_1 e_1) = m\omega^2 X_1(\lambda_1 e_1) = E_2 J_2 D^3 X_2(\lambda_2 0),$$

or

$$E_1 J_1 D^3 X_1(\lambda_1 e_1) = m\omega^2 X_2(\lambda_2 0) + E_2 J_2 D^3 X_2(\lambda_2 0); \tag{9}$$

- at the right end of the 2nd element:

$$X_2(e_2) = 0, \qquad D^2 X_2(e_2) = 0. \tag{10}$$

Substituting Eq. (7) into boundary conditions Eq. (8) it turns out that $a_1 = 0$, $c_1 = 0$. In the same way, the rest of conditions given by Eqs (9) and (10) lead to the set of algebraic equations and it may be written in the matrix form:

$$\mathbf{Ac} = \mathbf{0}, \tag{11}$$

where

$$\mathbf{A} = \begin{bmatrix} K_2(\lambda e_1) & K_4(\lambda e_1) & -K_1 & -K_2 & -K_3 & -K_4 \\ K_3(\lambda e_1) & K_1(\lambda e_1) & -K_2 & -K_3 & -K_4 & -K_1 \\ K_4(\lambda e_1) & K_2(\lambda e_1) & -K_3 & -K_4 & -K_1 & -K_2 \\ K'(\lambda e_1) & K''(\lambda e_1) & -K_4 & -K_1 & -K_2 & -K_3 \\ 0 & 0 & K_1(\lambda e_2) & K_2(\lambda e_2) & K_3(\lambda e_2) & K_4(\lambda e_2) \\ 0 & 0 & K_3(\lambda e_2) & K_4(\lambda e_2) & K_1(\lambda e_2) & K_2(\lambda e_2) \end{bmatrix} \tag{12}$$

and

$$K_\kappa = K_\kappa(0),$$
$$K'(\lambda e_1) = K_1(\lambda e_1) + \frac{m\omega}{(EJ\lambda^3)K_2(\lambda e_1)},$$
$$K''(\lambda e_1) = K_3(\lambda e_1) + \frac{m\omega}{(EJ\lambda^3)K_4(\lambda e_1)}.$$

The unknowns are collected in column matrix:

$$\mathbf{c} = [b_1, d_1, a_2, b_2, c_2, d_2]^{\mathrm{T}}. \tag{13}$$

To solve Eq. (11), one assumes that $\det \mathbf{A}(\lambda_\nu) = \mathbf{0}$ and it gives the set $\{\lambda_\nu\}$, $\nu = 1, 2, ..., n$. Based on a dispersion relationship one can calculated the frequency $\{\omega_\nu\}$ of the beam structure: $\omega_\nu^2 = \lambda_\nu^4 \gamma$.

Unknowns in matrix $\mathbf{c}$, Eq. (13), are

$$b_1 : d_1 : a_2 : ... = (-1)^{\alpha+1} M_{\alpha 1} : (-1)^{\alpha+2} M_{\alpha 2} : (-1)^{\alpha+3} M_{\alpha 3} : ..., \tag{14}$$

where $M_{\mu\kappa}$ is the minor of the $A_{\alpha\beta}$ element of the matrix $\mathbf{A}$, α and β are labels of the rows and columns, respectively.

Finally, the solution of Eq. (1) is given by:

$$X_\nu(x) = \begin{cases} b_1 K_2(\lambda_\nu x) + d_1 K_4(\lambda_\nu x), & x \in [0, x_m], \\ a_2 K_1(\xi_{\nu m}) + b_2 K_2(\xi_{\nu m}) + c_2 K_3(\xi_{\nu m}) + d_2 K_4(\xi_{\nu m}), & x \in (x_m, \ell], \end{cases} \tag{15}$$

where $\xi_{\mu m} = \lambda(x - x_m)$.

2.2. Forced vibration

Let be the excited force in Eq. (1) in the form Eq. (5). The solution to Eq. (1) is assumed as:

$$u(x,t) = X_f(x) \exp(i\omega_f t). \tag{16}$$

Substituting Eqs (5) and (16) to Eq. (1) one obtains:

$$EJD^4X_f(x) - \omega_f^2(\rho S + \alpha_m)X_f(x) = -f(x). \tag{17}$$

The solution to the above equation, i.e. forced vibrations, is given by:

$$X_f(x) = \sum_\nu C_\nu X_\nu(x), \quad \nu = 1, 2, ..., n, \tag{18}$$

where C_ν – any constant, $X_\nu(x)$ – Eq. (15).

After some calculation, constants C_ν are expressed (Brański, 2011):

$$C_\nu = \frac{1}{\omega_\nu^2 - \omega_f^2} G_\nu = \frac{1}{\alpha_\nu^2} G_\nu = \frac{1}{\rho S}\frac{1}{\alpha_\nu^2}\frac{1}{\beta_\nu^2} I_{\nu;f} = C_\nu^* I_{\nu;f}, \tag{19}$$

$$C_\nu^* = \frac{1}{\rho S}\frac{1}{\alpha_\nu^2}\frac{1}{\beta_\nu^2}, \qquad I_{\nu;f} = -\int_0^\ell f(x)X_\nu(x)\,\mathrm{d}x,$$
$$\omega_\nu^2 = \frac{EJ}{\rho S}\lambda_\nu^4, \qquad \beta_\nu^2 = \int_0^\ell X_\nu^2(x)\,\mathrm{d}x. \tag{20}$$

Thus, the problem of the beam vibration with concentrated mass, excited with the force $f(x,t)$ is solved. If the excited force is given by Eq. (5), in steady state $f(x) = f_0\delta(x - x_f)$, the $I_{\nu;f} = I_{\nu;0}$ and instead of Eq. (18) one has:

$$X_f(x) = \sum_\nu C_\nu^* I_{\nu;0} X_\nu(x) = \sum_\nu A_{\nu;0} X_\nu(x). \tag{21}$$

3. Beam vibration reduction by actuators

3.1. Beam vibration reduction by s-PZT

It is well known from (Hansen, Snyder, 1997; Fuller *et al.*, 1997; Brański, 2011; Przybyłowicz, 2002; Gosiewski, Koszewnik, 2007) and references cited therein, that the actuator-beam interacts approximately with moments of the couples of forces. Since the beam vibration equation is the forces equation, then to consider the action of the actuator on the beam, two moments are replaced with two couples of forces, Fig. 3. Next, the separate forces are taken into account in the Eq. (1). Hence, the total load is the sum of the load force expressed by Eq. (5) and the forces interacting between actuators and the beam, so it is given by:

$$f(x) = -f_0\delta(x - x_f) + [f_s\delta(x - x_{1s}) - 2f_s\delta(x - x_s) + f_s\delta(x + x_{2s})], \tag{22}$$

where $x_{1s} = x_s - \ell_s/2$, $x_{2s} = x_s + \ell_s/2$, x_s is the location of the actuator internal activity point; an expression in the square bracket is the sum of interacting forces actuators-beam.

To calculate $X_f(x)$, Eq. (18), the $A_{\nu;f}$ instead $A_{\nu;0}$, is calculated for $f(x)$ given by Eq. (22). Details of the solution may be found in (Brański, 2012), hence in explicit form:

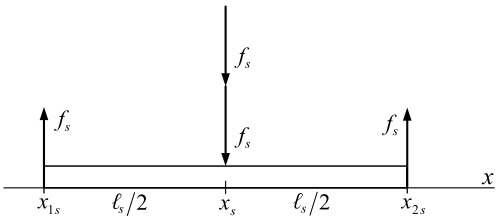

Fig. 3. External actuator pairs of forces with the same arms.

$$A_{\nu;f} = C_\nu^*\left(-f_0X_\nu(x_f) + \ell_s^2 f_s D^2X_\nu(x_s)\right) = A_{\nu;0} + A_{\nu;s}. \tag{23}$$

It should be noted that if the mode is symmetrical, then (Brański, 2011):

$$D^2X_\nu(x) = \pm\kappa s_{\nu;\max}. \tag{24}$$

The $\kappa s_{\nu;\max}$ is the maximum curvature of the mode $X_\nu(x)$ at the point $x = x_s$; $\kappa = D^2X/(1 + (DX)^2)^{3/2}$ (Fichtenholtz, 1999). The sign of the $\kappa s_{\nu;\max}$ is contractual, namely, if the bending of the beam is positive, the sign is positive and vice versa.

The reduction of the $A_{\nu;f}$ leads to the reduction of the beam vibration; a value zero of $A_{\nu;f}$ means the total reduction. Necessary condition for a minimum value of $A_{\nu;f}(x_s)$ is:

$$DA_{\nu;f}(x) = 0, \qquad x = x_s. \tag{25}$$

The point where the condition is satisfied is called a stationary point.

A sufficient condition of minimum of the $A_{\nu;f} = A_{\nu;f}(x_s)$ is

$$D^2A_{\nu;f} > 0, \qquad x = x_s. \tag{26}$$

From the system of Eqs (25) and (26), the x_s is calculated for which the amplitude $A_{\nu;f}(x_s)$ has a minimum value and therefore the reduction of vibrations is maximum. It should be recalled that in the case of symmetrical vibrations, the center of the s-PZT must be placed at the maximum curvature of the structure.

3.2. Beam vibration reduction by asymmetric actuator (a-PZT)

Now, let us take into account a-PZT with different arms, Fig. 4, i.e.:

$$M = f_s\ell_s = M_1 + M_2 = f_1\ell_1 + f_2\ell_2. \tag{27}$$

In this case, instead of Eq. (22), one has:

$$f(x) = -f_0\delta(x - x_f) + [f_1\delta(x - x_{1a}) - (f_1 + f_2)\delta(x - x_a) + f_2\delta(x - x_{2a})], \tag{28}$$

where $x_{1a} = x_a - \ell_1$, $x_{2a} = x_a + \ell_2$.

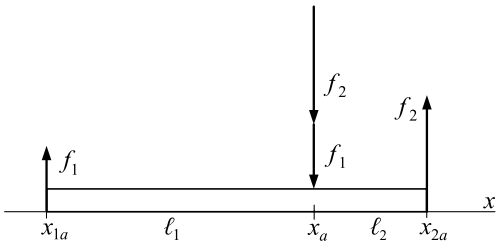

Fig. 4. External actuator pairs of forces with different arms.

In this case, $I_{\nu;f}$ in Eq. (20) is replaced by $I'_{\nu;f}$:

$$\begin{aligned} I'_{\nu;f} &= -\int_0^{\ell} f(x)X_\nu(x)\,\mathrm{d}x \\ &= -f_0X_\nu(x_f) + [f_1X_\nu(x_1) - (f_1+f_2)X_\nu(x_a) \\ &\quad + f_2X_\nu(x_2)] = -I_{\nu;0} + I'_{\nu;a}. \end{aligned} \tag{29}$$

Substituting Eq. (27) into square brackets and after some calculations one has:

$$\begin{aligned} &\frac{1}{\ell_2}f_1\left[\ell_2X_\nu(x_{1a}) - (\ell_1+\ell_2)X_\nu(x_a) + \ell_1X_\nu(x_{2a})\right] \\ &\qquad = \frac{\ell_1^2}{\ell_2}f_1D^2X_\nu(x_{1a}), \end{aligned} \tag{30}$$

where $D^2X_\nu(x_{1a})$ replace the forward finite difference (FFD) at the point x_{1a} (Quarteroni, 2009). To give the interpretation a technical character, first of all it should be noted that the bending moment of the beam is related with second derivative $D^2X_\nu(x_{1a})$, hence:

$$EJD^2X_\nu(x_{1a}) = M_\nu(x_{1a}). \tag{31}$$

In this way, based on Eq. (18), the problem of vibration reduction by asymmetrical PZT is solved.

Substituting Eq. (29) into Eq. (18), the reduction vibration is obtained:

$$\begin{aligned} X'_f(x) &= \sum_\nu C^*_\nu I'_{\nu;f}X_\nu(x) = \sum_\nu C^*_\nu\left(-I_{\nu;0} + I'_{\nu;a}\right)X_\nu(x) \\ &= \sum_\nu A'_{\nu;f}X_\nu(x), \end{aligned} \tag{32}$$

where, in explicit form,

$$\begin{aligned} A'_{\nu;f} &= C^*_\nu\left(-I_{\nu;0} + I'_{\nu;a}\right) \\ &= C^*_\nu\left(-f_0X_\nu(x_f) + \frac{\ell_1^2}{\ell_2}f_1\frac{M_\nu(x_{1a})}{EJ}\right) \\ &= A_{\nu;0} + A'_{\nu;a}. \end{aligned} \tag{33}$$

The reduction of the $A'_{\nu;f}$ leads to the reduction of the beam vibration; a value zero of $A'_{\nu;f}$ means the total reduction. So, quite similar like above, the $A'_{\nu;f}$ has minimum when $A'_{\nu;a}$ compensates $A_{\nu;0}$, but $A'_{f;\nu} \geq 0$.

Since $\ell_1 = x_a - x_{1a}$, $\ell_2 = x_{2a} - x_a = x_{1a} + \ell_s - x_a$ then instead of Eq. (33) one has:

$$\begin{aligned} A'_{\nu;f} &= C^*_\nu\left(-f_0X_\nu(x_f) + \frac{(x_a - x_{1a})^2}{(x_{1a} + \ell_a - x_a)}\frac{f_1}{EJ}M_\nu(x_{1a})\right) \\ &= A'_{\nu;f}(x_{1a}, x_a). \end{aligned} \tag{34}$$

Necessary conditions for a minimum value of $A'_{\nu;f}(x_{1a}, x_a)$ are:

$$\begin{aligned} DA'_{\nu;f}(x, x_a) &= 0, \qquad x = x_{1a} \\ DA'_{\nu;f}(x_{1a}, x) &= 0, \qquad x = x_a. \end{aligned} \tag{35}$$

A sufficient condition of minimum of the $A'_{\nu;f} = A'_{\nu;f}(x_{1a}, x_a)$ is:

$$D_1^2A'_{\nu;f}D_a^2A'_{\nu;f} - \left(D_1^2A'_{\nu;f}\right)^2 < 0, \tag{36}$$

where $D_1(\cdot) = D_{x_{1a}}(\cdot)$, $D_a(\cdot) = D_{x_a}(\cdot)$.

From the system of Eqs (35) and (36), the (x_{1a}, x_a) are calculated, for which the amplitude $A'_{\nu;f}(x_{1a}, x_a)$ has a minimum value and therefore the reduction of vibrations is maximum. Hence, the asymmetry of a-PZT is found. This way, the distribution and asymmetry of a-PZT were theoretically determined, ensuring maximum reduction of structure vibration.

Note, that in the case of asymmetrical vibrations, the a-point of the a-PZT must be placed at the maximum bending moment of the structure.

4. Reduction effectiveness coefficients

The effect of PZT acting is measured by the reduction of three parameters, i.e. the vibration, bending moment, and shear force. However, it should be noted that the reduction of amplitude of vibrations translates into the reduction of these parameters. Therefore, it is enough to present the amplitude vibration reduction. To determine the reduction of the amplitude, the reduction coefficient is formulated:

$$R_{\nu;A} = \frac{A_{\nu;0} - A_{v;f}}{A_{\nu;0}} \cdot 100\%, \tag{37}$$

where $A_{\nu;0}$ – vibration amplitude without PZT; the vibration is excited only by $f_0(x_f)$, $A_{v;f}$ – vibration amplitude with PZT; the vibration is excited only $f_0(x_f)$ and reduced by PZT. The coefficient $R_{\nu;A}$ is the first measure of the vibration reduction; hence next reduction coefficients follow, i.e. mode $R_{\nu;X}$, bending moment $R_{\nu;M}$, and shear force $R_{\nu;Q}$. Forms of these coefficients are the same like Eq. (44) and they are obvious.

5. Analytical and numerical calculations

To justify the utility of a-PZT and demonstrate its advantage over s-PZT, measured via R_A, following groups of researches are performed:

1) center of s-PZT is changed,
2) asymmetry and a-point of a-PZT are changed.

In both cases, the objective functions are formulated and optimal solutions are obtained by minimizing them. All calculations are performed separately for the first three modes $\{X_\nu\} = \{X_1, X_2, X_3\}$.

In calculations the following data are assumed:

$$\ell = 1 \text{ m}, \qquad \rho = 2700 \text{ kg} \cdot \text{m}^{-3},$$
$$S = 2.5 \cdot 10^{-4} \text{ m}^2, \qquad \text{E} = 69 \cdot 10^9 \text{ Pa},$$
$$h_1 = 0.05 \text{ m}, \qquad h_2 = 0.005 \text{ m},$$
$$J = (h_1 h_2^3)/12 \text{ m}^4, \qquad x_m = 0.39\ell,$$
$$\gamma = 53.2407 \text{ m}^4 \cdot \text{s}^{-2}.$$

Next, based on equation $\det \mathbf{A}(\lambda_\nu) = 0$, the set of eigenvalues $\{\lambda_\nu\}$ are calculated and

$$\{\lambda_\nu\} = \{2.7121,\ 5.9945,\ 9.1517,\ 11.6305,\ 15.6784,\ ...\}.$$

Hence

$$\{\omega_\nu\} = \{53.6686,\ 262.1975,\ 611.1207,\ 987.0076,\ 1793.6011,\ ...\}.$$

Based on the Eq. (15), shapes of the first three modes are shown in Fig. 5. The figure shows that all modes are asymmetrical. The length of all actuators is the same, $\ell_s = 0.2\ell$, f_0 – the amplitude of the excited force is chosen by empirical way to obtain meaningful deflections of separate modes: $\{f_{0;\nu}\} = \{f_{0;1}, f_{0;2}, f_{0;3}\} = \{0.15,\ 0.8,\ 2\}$ N, $m = 0.3$ kg – concentrated mass is distributed on the each modes as follow: $\{x_{m;\nu}\} = \{x_{m;1}, x_{m;2}, x_{m;3}\} = \{0.39,\ 0.85,\ 0.45\} \cdot \ell$.

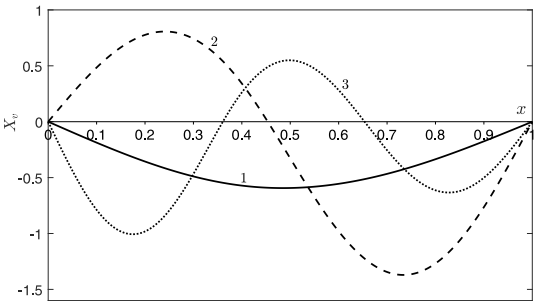

Fig. 5. Eigenfunctions (modes): 1 – X_1, 2 – X_2, 3 – X_3.

5.1. Vibration reduction via s-PZT

With a fixed length ℓ_s and fixed energy added to BMA by s-PZT, only the s-PZT centre is optimized. For each mode X_ν, the goal function is $A_{\nu;f}(x_s)$, Eq. (23). By minimizing $A_{\nu;f}(x_s)$, an optimal position s-PZT expressed by $x_{s;\nu}$ is obtained. A necessary condition for minimum value of $A_{\nu;f}(x_s)$ is given by Eq. (25), hence:

$$DA_{\nu;f}(x) = \ell_s^2 \frac{f_s}{EJ} DM_\nu(x) = 0, \qquad x = x_s, \qquad (38)$$

where the Eq. (31) is taken into account.

A sufficient condition of minimum of the $A_{\nu;f}(x_s)$ is given by Eq. (26), hence $D^2 M_\nu(x) > 0$, $x = x_s$. First of all, the bending moments $M_\nu(x)$ of separate modes are calculated, Fig. 6. Then, based on the necessary condition, Eq. (38), and sufficient one, $x_{s;\nu}$ are found.

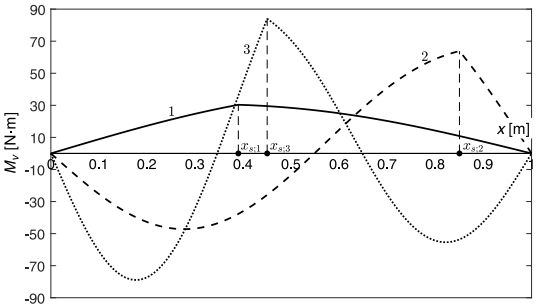

Fig. 6. Bending moments $M_\nu(x)$ of the modes: $\{M_\nu\} = \{M_1,\ 0.5M_2,\ 0.5M_3\}$.

As a result, optimal positions of s-PZT expressed by the internal activity point $x_{s;\nu}$ are obtained, namely: $\{x_{s;\nu}\} = \{x_{s;1},\ x_{s;2},\ x_{s;3}\} = \{0.39,\ 0.85,\ 0.45\}$.

5.2. Vibration reduction via a-PZT

For a-PZT length and an energy added by a-PZT to BMA, are the same like for s-PZT for each mode, respectively. Hereunder, the a-PZT position on the beam, expressed by x_a, and its asymmetry, expressed by x_{1a} or x_{2a}, here x_{1a}, are calculated. Exact values of x_a and x_{1a} can be found from Eqs (35) and (36). But here the optimization problem is solved numerically, where the goal function is $A'_{\nu;f}(x_{1a}, x_a)$, Eq. (34). By minimizing $A'_{\nu;f}(x_{1a}, x_a)$, an optimal position x_a and asymmetry, here expressed by x_{1a}, are obtained. Results are presented in Fig. 7, where red solid points show the x_a and x_{1a} values calculated by Eqs (35) and (36). Based on Eqs (35) and (36), these problems are solved numerically; results are shown in Fig. 7.

5.3. Efficiency of vibration reduction

First, the distribution of s-PZT (red) and a-PZT (blue) on separate modes is shown in Fig. 8. The distribution of s-PZT and a-PZT is the same and is given by $\{x_{s;1},\ x_{s;2},\ x_{s;3}\} = \{x_{a;1},\ x_{a;2},\ x_{a;3}\} = \{0.39,\ 0.85,\ 0.45\}$ m. Figure 8 shows the effect of active vibration reduction via separate PZTs.

Figure 8 shows that separate $x_{s;\nu}$ points indicate centres of s-PZTs, but the same points indicate a-PZTs asymmetry and this asymmetry is strictly specified. Furthermore, the efficiency of a-PZT is greater than that of s-PZT; quantitative results are presented in the Table 1.

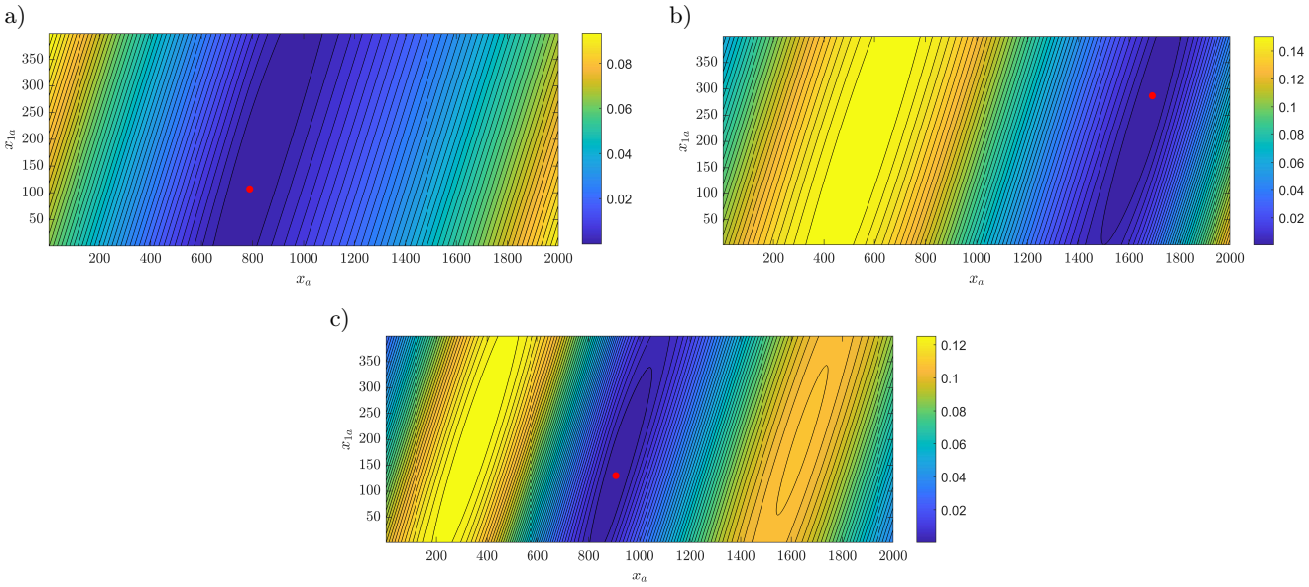

Fig. 7. a) The $A'_{\nu;f} = A'_{\nu;f}(x_1, x_a)$ for the first mode shape; b) the $A'_{\nu;f} = A'_{\nu;f}(x_1, x_a)$ for the second mode shape, c) the $A'_{\nu;f} = A'_{\nu;f}(x_{1a}, x_a)$ for the third mode shape.

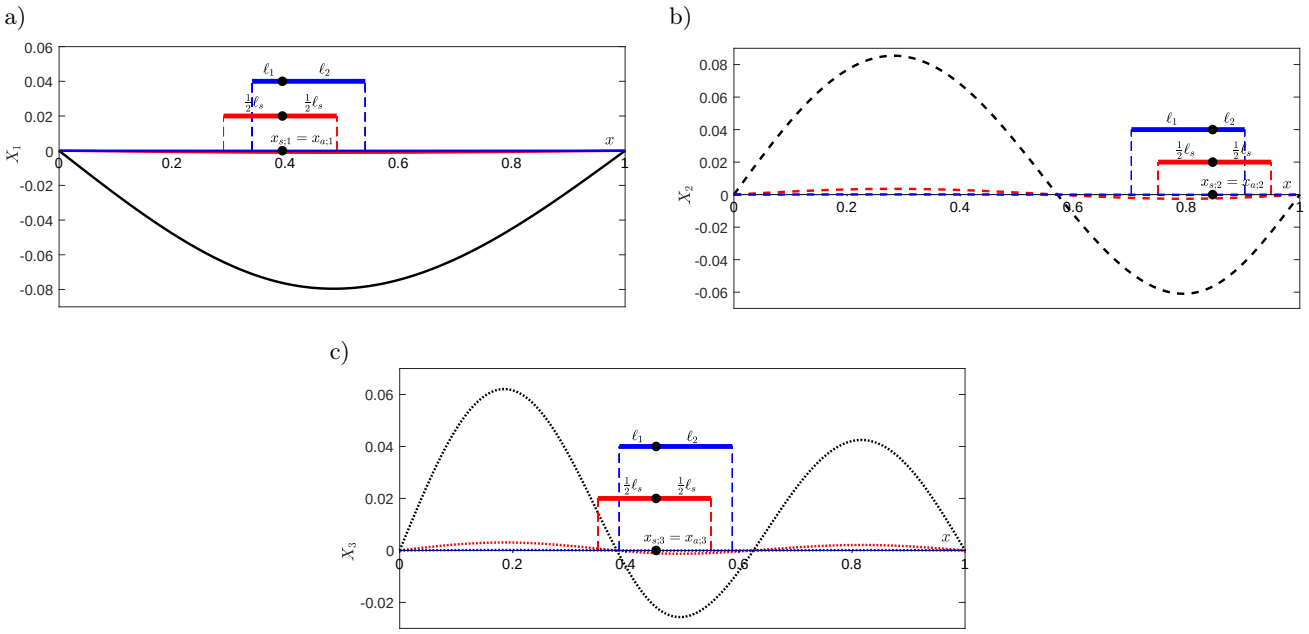

Fig. 8. Undamped mode (black), after acting s-PZT (red) and a-PZT (blue): a) first mode shape, b) second mode shape, c) third mode shape.

Table 1. Mode reduction coefficient $R_{\nu;X}$, $\ell_s = 0.2$ m.

	s-PZT			a-PZT			
	f_s [N]	x_s [m]	$R_{\nu;X}$ [%]	$\{f_1, f_2\}$ [N]	$\{\ell_1, \ell_2\}$ [m]	x_a [m]	$R_{\nu;X}$ [%]
X_1	1.3830	0.39	98.50	{2.9551, 0.9027}	{0.0468, 0.1532}	0.39	99.89
X_2	1.3800	0.85	95.74	{0.9256, 2.7112}	{0.1491, 0.0509}	0.85	99.82
X_3	1.0900	0.45	94.93	{1.8167, 0.7786}	{0.0600, 0.1400}	0.45	99.71

5.4. LQR controller design

Simulating the LQR control algorithm requires first deriving state space equations which were constructed from the equations of motion as (Parameswaran *et al.*, 2015; Le, 2009):

$$\dot{\mathbf{x}} = \mathbf{A}\mathbf{x} + \mathbf{B}\mathbf{u}, \tag{39}$$

$$\mathbf{y} = \mathbf{C}\mathbf{x}, \tag{40}$$

where $\mathbf{x}$ – state vector, $\mathbf{y}$ – output vector, $\mathbf{u}$ – input vector, $\mathbf{A}$ – system matrix, $\mathbf{B}$ – control matrix, $\mathbf{C}$ – output matrix.

Minimizing the cost function:

$$\mathbf{J} = \int_0^\infty \left(\mathbf{y}^{\mathrm{T}}\mathbf{Q}\mathbf{y} + \mathbf{u}^{\mathrm{T}}\mathbf{R}\mathbf{u}\right) \mathrm{d}t, \tag{41}$$

leads to obtaining a control gain of the LQR. $\mathbf{Q}$ and $\mathbf{R}$ are the power matrices. System input signal is defined as $\mathbf{u} = -\mathbf{R}^{-1}\mathbf{B}^{\mathrm{T}}\mathbf{P}\mathbf{x}$ where $\mathbf{P}$ is the solution of the Riccati equation (Zhang, Schmidt, 2012). The LQR controller was designed for both s-PZT and a-PZT with the following data:

$$\mathbf{A} = \begin{bmatrix} 0 & 1 \\ -\omega_\nu^2 & 0 \end{bmatrix}, \tag{42}$$

$$\mathbf{B}_{\text{s-PZT}} = k_a \begin{bmatrix} X_\nu(x_{1s}) - 2X_\nu(x_s) + X_\nu(x_{2s}) \\ 0 \end{bmatrix}, \tag{43}$$

$$\mathbf{B}_{\text{a-PZT}} = k_a \frac{\ell_s}{2\ell_1\ell_2} \cdot \begin{bmatrix} \ell_2 X_\nu(x_{1a}) - (\ell_1+\ell_2)X_\nu(x_a) + \ell_1 X_\nu(x_{2a}) \\ 0 \end{bmatrix}, \tag{44}$$

$$\mathbf{C} = \frac{k_s}{c_s b_s (x_{t2} - x_{t1})} \begin{bmatrix} X'_\nu(x_{t2}) - X'_\nu(x_{t1}) \\ 0 \end{bmatrix}, \tag{45}$$

where $k_a = \frac{1}{2}\frac{Ed_{31}(h_2+h_a)}{\rho S(1+mX_\nu(x_m))}$, h_a is thickness of the actuators, $h_a = 0.005$ m, d_{31} is piezoelectric coefficient for PZT-5H, $d_{31} = -320 \cdot 10^{-12}$ m/V, $k_s = -b_s\left(h_s + h_2/2\right)\left(k_{31}^2/g_{31}\right)$, x_{t1}, x_{t2} are coordinates of the sensor edges, b_s is length of the sensor, $b_s = 0.1$ m, h_s is thickness of the sensor, $h_s = 0.005$ m, k_{31} is coupling coefficient for PZT-5H, $k_{31} = 0.44$, g_{31} is piezoelectric coefficient for PZT-5H, $g_{31} = -9.5 \cdot 10^{-3}$ V/m, c_s is capacitance per unit area of the sensor $c_s = 400 \cdot 10^{-9}$ F/cm^2.

Data for the power matrices was chosen as:

$$\mathbf{Q} = \begin{bmatrix} 1.8625 \cdot 10^4 & 0 \\ 0 & 0 \end{bmatrix}, \qquad \mathbf{R} = \{R_1,\ R_2,\ R_3\} = \{0.1,\ 1,\ 1\}. \tag{46}$$

Figures 9–11 show the effect of s-PZT and a-PZT in the time domain.

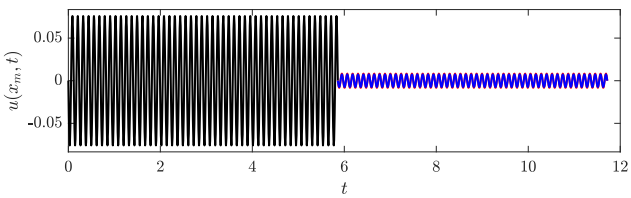

Fig. 9. Before vibration reduction (black), after acting s-PZT (red) and a-PZT (blue); first mode shape.

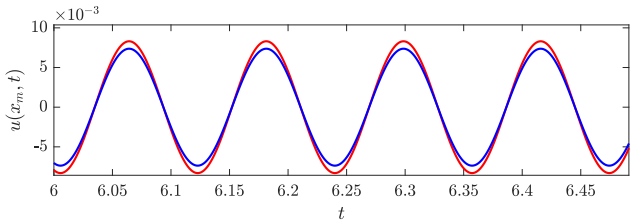

Fig. 10. A zoomed part of Fig. 9 for the first mode shape; s-PZT (red), a-PZT (blue).

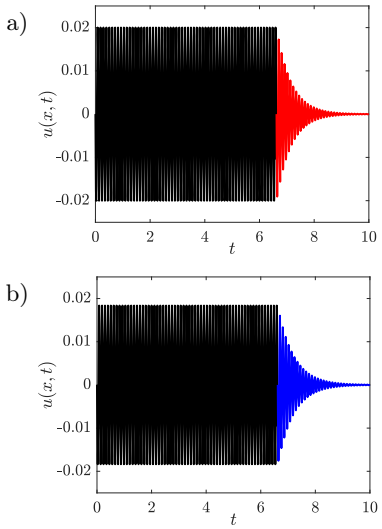

Fig. 11. (a) Open-loop s-PZT (black), closed-loop s-PZT (red); (b) open-loop a-PZT (black), closed-loop a-PZT (blue); first mode shape.

The Table 1 shows that the vibration reduction efficiency with s-PZT, measured by mode reduction coefficients $R_{\nu;X}$, decreases with increasing the mode number.

6. Conclusions

The article presented the exact theory of the active vibration reduction of asymmetrical beam vibrations. To achieve this, the a-PZT was worked out and located at the point of the beam with the maximum bending moment. This made it possible to formulate the criterion of the maximum bending moment to obtain the optimal solution to such a problem. Quantitatively it was justified that under the same geometrical and physical conditions, the a-PZT provides better efficiency than standard s-PZT. Based on the exact formulations and numerical considerations, the following conclusions, can be enumerated:

1) The criterion of the maximum bending moment solves the problem of the optimal vibration reduction of asymmetric beam vibrations.
2) The criterion shows the asymmetry of a-PZT and its position on the beam; all optimization parameters are strictly defined.

3) The a-PZT reduces vibrations more effectively than the s-PZT assuming that the dimensions of both actuators and the amount of energy added to the system is the same in both cases.

The results of the paper can be used directly in practice or be a reference point for further considerations, i.e. to reduce vibration of other one-dimensional structures. In next studies, the idea of criterion of the maximum bending moment will be used to active reduction of vibrations of two-dimensional asymmetrical structures.

Declarations

Funding

No funds, grants, or other support were received.

Conflicts of interest

The Authors declare that there is no conflict of interest.

References

1. Augustyn E., Kozień M.S., Prącik M. (2014), FEM analysis of active reduction of torsional vibrations of clamped-free beam by piezoelectric elements for separated mode, *Archives of Acoustics*, **39**(4): 639–644, doi: 10.2478/aoa-2014-0069.

2. Barboni R., Mannini A., Fantini E., Gaudenzi P. (2000), Optimal placement of PZT actuators for the control of beam dynamics, *Smart Materials and Structures*, **9**: 110–120, doi: 10.1088/0964-1726/9/1/312.

3. Brand Z., Cole M.O.T. (2020), Controllability and actuator placement optimization for active damping of a thin rotating ring with piezo-patch transducers, *Journal of Sound and Vibration*, **472**: 115172, doi: 10.1016/j.jsv.2020.115172.

4. Brański A. (2011), An optimal distribution of actuators in active beam vibration – some aspects, theoretical considerations, [in:] *Acoustic Waves – From Microdevices to Helioseismology*, Beghi M.G. [Ed.], pp. 397–418, IntechOpen, Rijeka.

5. Brański A. (2012), Modes orthogonality of mechanical system simple supported beam-actuators-concentrated masses, *Acta Physica Polonica A*, **121**(1A): 126–131.

6. Brański A. (2013), Effectiveness analysis of the beam modes active vibration protection with different number of actuators, *Acta Physica Polonica A*, **123**(6): 1123–1127, doi: 10.12693/APhysPolA.123.1123.

7. Brański A., Lipiński G. (2011), Analytical determination of the PZT's distribution in active beam vibration protection problem, *Acta Physica Polonica A*, **119**(6A): 936–941.

8. Dhuri K.D., Seshu P. (2006), Piezo actuator placement and sizing for good control effectiveness and minimal change in original system dynamics, *Smart Materials and Structures*, **15**(6): 1661–1672, doi: 10.1088/0964-1726/15/6/019.

9. Fawade A.S., Fawade S.S. (2016), Modeling and analysis of vibration controlled cantilever beam bounded by PZT Patch, *International Journal of Engineering Inventions*, **5**(7): 7–14.

10. Fichtenholtz G.M. (1999), *Differential and Integral Calculus*, PWN, Warsaw.

11. Filipek R., Wiciak J. (2008), Active and passive structural acoustic control of the smart beam, *The European Physical Journal Special Topics*, **154**: 57–63, doi: 10.1140/epjst/e2008-00517-2.

12. Fuller C.R., Elliot S.J., Nielsen P.A. (1997), *Active Control of Vibration*, Academic Press, London.

13. Gosiewski Z., Koszewnik A. (2007), The influence of the piezoelements placement on the active vibration damping system, [in:] *Proceedings of the 8th Conference on Active Noise and Vibration Control Methods*, pp. 69–79, Kraków, Poland.

14. Gupta V., Sharma M., Thakur N. (2011), Mathematical modeling of actively controlled piezo smart structures: a review, *Smart Structures and Systems*, **8**(3): 275–302, doi: 10.12989/sss.2011.8.3.275.

15. Hansen C.H., Snyder S.D. (1997), *Active Control of Noise and Vibration*, E&FN SPON, London.

16. Hu K.M., Li H. (2018), Multi-parameter optimization of piezoelectric actuators for multi-mode active vibration control of cylindrical shells, *Journal of Sound and Vibration*, **426**: 166–185, doi: 10.1016/j.jsv.2018.04.021.

17. Kaliski S. (1986), *Vibrations and Waves* [in Polish], PWN, Warszawa.

18. Kasprzyk S., Wiciak M. (2007), Differential equation of transverse vibrations of a beam with a local stroke change of stiffness, *Opuscula Mathematica*, **27**(2): 245–252.

19. Khasawneh F.A., Segalman D. (2019), Exact and numerically stable expressions for Euler-Bernoulli and Timoshenko beam modes, *Applied Acoustics*, **151**: 215–228, doi: 10.1016/j.apacoust.2019.03.015.

20. Kozień M.S. (2013), Analytical solutions of excited vibrations of a beam with application of distribution, *Acta Physica Polonica A*, **123**(6): 1029–1033, doi: 10.12693/APhysPolA.123.1029.

21. Le S. (2009), *Active vibration control of a flexible beam*, Master's Thesis, Mechanical and Aerospace Engineering, San Jose State University, doi: 10.31979/etd.r8xg-waar.

22. Parameswaran A.P., Ananthakrishnan B., Gangadharan K.V. (2015), Design and development of a model

free robust controller for active control of dominant flexural modes of vibrations in a smart system, *Journal of Sound and Vibration*, **355**: 1–18, doi: 10.1016/j.jsv.2015.05.006.

23. Przybyłowicz P.M. (2002), *Piezoelectric Vibration Control of Rotating Structures*, Scientific works of the Warsaw University of Technology. Mechanics, Vol. 197, Oficyna Wydawnicza Politechniki Warszawskiej, Warszawa.

24. Quarteroni A. (2009), *Numerical Models for Differential Problems*, Springer-Verlag, Milan.

25. Yassin B., Lahcen A., Zeriab E. (2018), Hybrid optimization procedure applied to optimal location finding for piezoelectric actuators and sensors for active vibration control, *Applied Mathematical Modelling*, **62**: 701–716, doi: 10.1016/j.apm.2018.06.017.

26. Zhang S.Q., Schmidt R. (2012), LQR control for vibration suppression of piezoelectric integrated smart structures, *Proceedings in Applied Mathematics and Mechanics*, **12**(1): 695–696, doi: 10.1002/pamm.201210336.

27. Zhang X., Takezawa A., Kang Z. (2018), Topology optimization of piezoelectric smart structures for minimum energy consumption under active control, *Structural and Multidisciplinary Optimization*, **58**: 185–199, doi: 10.1007/s00158-017-1886-y.

28. Zorić N.D., Tomović A.M., Obradović A.M., Radulović R.D., Petrović G.R. (2019), Active vibration control of smart composite plates using optimized self-tuning fuzzy logic controller with optimization of placement, sizing and orientation of PFRC actuators, *Journal of Sound and Vibration*, **456**: 173–198, doi: 10.1016/j.jsv.2019.05.035.